VITAE, REVISTA DE LA FACULTAD DE CIENCIAS FARMACÉUTICAS Y ALIMENTARIAS
ISSN 0121-4004 / ISSNe 2145-2660. Volumen 22 número 1, año 2015
Universidad de Antioquia, Medellín, Colombia. págs. 13-26.
DOI: http://dx.doi.org/10.17533/udea.vitae.v22n1a02

MURINE INVARIANT NATURAL KILLER T CELLS RECOGNIZE GLYCOLIPIDS DERIVED FROM EXTRACTS OF THE LICHEN *Stereocaulon ramulosum*

CÉLULAS T ASESINAS NATURALES INVARIANTES MURINAS RECONOCEN GLICOLIPIDOS DERIVADOS DE EXTRACTOS DEL LIQUEN *Stereocaulon ramulosum*

Andres BAENA, M.Sc, Ph.D.[1, 2, *], Lina GOMEZ-GIRALDO, B.Sc.,[1, 3] Wilton A. GOMEZ, B.Sc.[1, 3]
Carlos A. PELAEZ, M.Sc, Ph.D.[4]

Recibido: Febrero 06 de 2015. Aceptado: Mayo 05 de 2015.

ABSTRACT

Background: Invariant natural killer T cells (iNKT) can be activated by certain types of glycolipids that have the potential to generate adjuvant effects which could be used to develop effective and safe immunotherapies. Many of these glycolipids have been isolated from natural organisms, but there is a great amount of these organisms completely unexplored as a source of these types of compounds. Some of these organisms are lichens which are complex symbiotic organisms that have been showed to contain glycolipids. **Objectives:** We decide to test if glycolipids isolated from lichens would be able to activate iNKT cells in vitro and in vivo. **Methods:** We have used extracted glycolipids from 43 different species of lichens from Colombia. We have used iNKT hybridoma cells, C57BL/6 mice, IL-2 ELISA and the B16 melanoma to test for the adjuvant capabilities of glycolipids isolated from lichens. **Results:** In this study we have found two glycolipids with the capacity to activate iNKT cells *in vitro*. One of the glycolipids was able to activate iNKT cells *in vivo*, and was competent to induce protection against the B16 melanoma in the mouse model. **Conclusions:** We propose a possible chemical structure for a novel glycolipid called β-GalCer-lich (**1**) derived from the lichen *Stereocaulon ramulosum*.

Keywords: iNKTs; Glycolipids; CD1d; Lichens; Adjuvant

RESUMEN

Antecedentes: Las células asesinas naturales T (iNKT) pueden ser activadas por ciertos tipos de glicolípidos que tienen el potencial para generar efectos adyuvantes los cuales pueden ser usados para desarrollar inmunoterapias efectivas. Muchos de estos glicolípidos han sido aislados de organismos naturales, pero hay una gran cantidad de organismos completamente inexplorados como fuente de este tipo de compuestos. Algunos de estos organismos son los líquenes, los cuales son organismos simbiontes complejos para los que se ha mostrado que contienen glicolípidos. **Objetivos:** Nosotros decidimos probar

[1] Grupo de Inmunología Celular e Inmunogenética GICIG, Departamento de Microbiología y parasitología, Facultad de Medicina, Universidad de Antioquia UdeA, Calle 70 No.52-21, Medellín, Colombia

[2] Sede de Investigación Universitaria, Facultad de Medicina, Universidad de Antioquia, Cra. 53 No. 61-30, Lab 510, Medellín-Colombia

[3] L.G.G and W.G.G contributed equally to the development of this work

[4] Grupo Interdisciplinario de estudios moleculares GIEM, Departamento de Microbiología y parasitología, Facultad de Medicina, Universidad de Antioquia UdeA, Calle 70 No.52-21, Medellín, Colombia

[*] Corresponding author: andres.baenag@udea.edu.co

si los glicolípidos aislados de líquenes podrían ser capaces de activar alas celulas iNKT in vitro e in vivo. **Metodos:** Nosotros hemos extraído glicolípidos de 43 especies de líquenes de Colombia. Nosotros hemos usado células de un hibridoma de iNKTs, ratones C57BL/6, ELISA para IL-2 y el melanoma B16 para probar la capacidad adyuvante de los glicolipidos aislados de los líquenes. **Resultados:** En este estudio nosotros hemos encontrado dos glicolípidos con la capacidad de activar iNKTs *in vitro*. Uno de los glicolípidos fue capaz de activar células iNKT *in vivo*, y fue competente para inducir protección contra el melanoma B16 en el modelo de ratón. **Conclusiones:** Nosotros proponemos una posible estructura química para el nuevo glicolípido llamado β-GalCer-lich (**1**) derivado del liquen *Stereocaulon ramulosum*.

Palabras clave: iNKTs; Glicolípidos; CD1d, Líquenes; Adyuvante

INTRODUCTION

Invariant natural killer T cells (iNKT) are defined as T cells that express NK lineage markers in addition to semi-invariant CD1d-restricted αβ TCRs (Vα14-Jα18/Vβ8, Vβ7, and Vβ2 in the mouse or Vα24-Jα18/Vβ11 in human) (1, 2). iNKT cells can secrete a large variety of cytokines to different glycolipid antigens presented by the CD1d molecule, which have been showed to influence the immune response in multiple infection diseases. In recent years different new glycolipid antigens has been identified, many of which have the potential to generate adjuvant effects that enhance the activity of adaptive immune cells such as dendritic cells (DCs), T cells and B cells (3, 4). Moreover, for certain diseases such as tuberculosis, malaria and AIDS, it will be important to find better glycolipid adjuvants so we could improve new vaccine candidates for these public health problems (5, 6). Most of the glycolipid adjuvants that are available were initially derived from single natural organisms. Today we have a great diversity of organisms that contain glycolipids with the potential to activate iNKT cells that still remain unexplored (7). Lichens are one of the best examples of organisms that contain a great diversity of glycolipids (8, 9). The glycolipid composition varies between different species of lichens and some examples of these glycolipids are: monogalactosyldiacylglycerol (MGD), digalactosyldiacylglycerol (DGD), trigalactosyldiacylglycerol (TGD), lyso-TGD (Sn-1 and Sn-2), sulfoquinovosyldiacylglycerol (SQDG) and lyso-SQDG (Sn-1 and Sn-2) (10-13). Moreover, the fatty acid part of these glycolipids has showed a great diversity in their carbon and saturation number that is spread and enriched among different types of lichens. For this reasons we decide to look if glycolipids isolated from lichens have the capacity to activate iNKT cells.

It is very interesting that αGalCer, which is the most potent compound known to activate iNKT cells (14), was isolated presumably from a cyanobacteria algae (present in a marine sponge) that is closely related to the algae present in lichens (4, 15, 16). Lichens are symbiotic organisms consisting of a fungus and cyanobacteria algae that have been used in traditional medicine for the treatment of diseases such as tuberculosis (17, 18). Moreover, there are different reports in which lichen extracts have been showed to have anticancer and antibiotic properties (19-21).

The fact that Colombia is one of the countries with the highest diversities of lichens in the world, with approximately 1500 species, allow us to obtain good number of lichen samples (22, 23). In this study we have isolated glycolipids from 43 different species of lichens and found 2 of them with the capacity to activate iNKT cells *in vitro*. As we shown in this paper, the glycolipid extracted from *Stereocaulon ramulosum* (*S.ramulosum*) was able to activate iNKT cells *in vivo* and confered protection as an adjuvant in the mouse model against the B16 melanoma. Finally, we propose a possible chemical structure for the glycolipid isolated from *S. ramulosum* that could be produced synthetically in the near future as a potential vaccine adjuvant.

METHODS

Mice

All mice used in the study were purchased from Jackson Laboratories (Bar Harbor, ME). C57BL/6 female mice were maintained under specific pathogen-free conditions and were used for experiments at 6-8 weeks of age. All procedures involving animals were approved by the Institutional Animal Care and Use Committee of the Universidad de Antioquia.

Cell culture

For in vitro cultured, murine cells were maintained in complete RPMI-1640 medium (Invitrogen, Carlsbad), supplemented with 10 mM HEPES pH 7.5, 1% L-glutamine, 1% nonessential amino acids, 1% Sodium Pyruvate 55 μM 2-mercaptoethanol, 20 μg/ml gentamicin (Gibco), 10% heat-inactivated fetal calf serum (FCS) and beta-mercapto-ethanol. The cell lines were maintained in an incubator with a humidified atmosphere containing 5 % CO2 at 37°C.

Bone Marrow-Derived Dendritic Cells (BMDCs)

Murine BMDCs were prepared following the Lutz protocol (24). Briefly, the bone marrow progenitors were obtained from flushed femurs and tibias with complete media using a 25-G needle. The suspension was passed through a 70-μm-nylon cell strainer to disperse clumps. The red cells were lysed using the RBC lysis buffer (Sigma). The cells were then re-suspended in conditional media (complete media plus 20 ng/ml of GM-CSF from Peprotech) and growth in 100-mm culture plates. Every two days, half of the media was replaced with fresh conditional media. At the 10th day of culture the non-adherent cells were removed from the plates and centrifuged for 10 min at 1500 rpm. Finally, the cells were count and frozen down in liquid nitrogen at $5x10^5$ cells /vial.

iNKT cell hybridoma Stimulation

For dose titration experiments, BMDCs and DN3A4-1.2 NKT hybridomas (M. Kronenberg at La Jolla Institute for Allergy and Immunology and S.A. Porcelli at the Albert Einstein College of Medicine) were cultured at a 2:1 hybridoma:BMDC ratio (murine iNKT hybridoma cells at $5x10^4$ cells/well in 96-well plates were stimulated with the $1x10^5$ cells/well pulsed BMDCs with the indicated doses of glycolipids) in the presence of 0.5 mg/ml LPS (Escherichia coli O26:B6; Sigma-Aldrich). Supernatants were harvested after 16 h at 37°C, and levels of murine IL-2 secretion were determined in the supernatants by ELISA. To block antigen presentation we use the anti-CD1d 1B1 (BD Biosciences) antibody that was added to the BMDCs at 10 ug/ml 30 min before addition of the iNKT cells and after 24hrs the supernatant was tested for IL-2 production by ELISA.

Reagents and glycolipids

Glycolipids were prepared as solutions for injection in vehicle (PBS with 0.1 % DMSO and 0.05 % of Tween-20). For in vitro assays, glycolipids were dissolved in 10 % DMSO at 500 mM, sonicated in a water bath sonicator for 5 min and then diluted directly into prewarmed (37°C) culture medium at a final concentration of 20 ng/ul. Glycolipid MGDG and αGalCer were purchased from Avanti Polar Lipids and Funakoshi co., respectively. The αGalCer was used as a positive control at a final concentration of 100 ng/ml and DMSO was used as a negative control for all the in vitro experiments.

Lichens collection

The lichens were collected in the following locations: Barbosa, Antioquia-Colombia (N 06° 27.421'W 0.75° 18.22'; 1300 mts), Santa Elena, Antioquia-Colombia (N 06° 15.821´W 0.75° 29.465´; 2325 mts), Envigado, Antioquia-Colombia (N 06° 16.061´ W 0.75° 29.682´; 2400 mts) and Belmira, Antioquia-Colombia (N06°31.957´ O 075° 38.662´; 2800 mts). We collected approximately 20 gr of 43 different species of lichens, for which a representative piece of each sample was dried and stored in a small collection, which was used to stablish the lichens classifications. Each sample was accompanied by a set of photographs as evidence of the place where the sample was found and also to check for taxonomic details of the fresh sample; the rest of the material was used for the glycolipid extraction.

Glycolipid extraction

The lichens were washed multiple times with water and purified from contaminants using tweezers and then they were left at room temperature for 24 hrs. After this step, the lichens were completely dried in an oven at 105 °C overnight. The samples were blended to get a particulate material to optimize the extraction. All the glycolipids were extracted with CH_2Cl_2:MeOH: ddH_2O (1:2:1) in a shaker for 24 hrs as a modification of the Bligh and Dyer protocol (*25*). The liquid phase was separated from the particulate material. The samples were re-extracted with CH_2Cl_2:MeOH: ddH_2O (1:1:1) for 7 hrs and then the phases were allowed to separate for 18 hrs before the lower dichloromethane was removed and filtered through Whatman filter paper and dried with nitrogen gas. Finally, the samples were store in sterile glass containers at room temperature and in the dark.

For the soxhlet extraction the material was refluxed over the thimble in a standard soxhlet extraction apparatus for 3 hrs using Hexane, chloroform and methanol. The glycolipid containing solvent

was then recovered in the attached round-bottom flask which was used to dry the lipid under rotary vacuum evaporation (<37 °C). The glycolipid residue was re-dissolved, transferred to a sterile small glass container, and then solved evaporated.

ELISA

Supernatant levels of IL-2 were measured by ELISA using capture and biotinylated detection antibody pairs and streptavidin–horseradish peroxidase (BD PharMingen) with substrate reagent pack (R&D). IL-2 standard was obtained from Pepro-Tech (Rocky Hill, NJ). 96 well plates were coated overnight at 4 °C with the capture antibody and blocked for nonspecific binding sites by adding 1 % bovine serum albumin in phosphate-buffered saline (PBS) for 1 hr. The supernatants were added for 2 hrs and then the detection biotnylated antibody was added for 1hr. After these the streptavidine-HRP was added for 45 min. Finally, the substrate was added and the reaction was stopped with sulfuric acid. All the washes were done with PBS 1X and 0.05 % of Tween 20. Optical density at 450 nm was measured 5 minutes after stopping the reaction. The IL-2 concentrations were calculated based on the standard curve obtained in each assay (Supl. Fig. 2A, 2B, 2C and 2D) (All Supplementary material are presented at the end of the paper).

TLC (Thin layer chromatography)

The crude extract was dissolved in a minimum amount of CH_2Cl_3:MeOH (2:1) and , applied to a 5 mm preparative TLC silica plates (Alltech Associates) and eluted with CHCl3:MeOH:AcOH:H2O (100:20:12:5). The plate was divided into three section based on polarity (top, S5 middle, and bottom). Each section was scraped off the plate and extracted with CHCl3:MeOH (5:1). The resulting solution was concentrated and further purified by preparative TLC (0.5 mm): the top section was eluted in CH_2Cl_3:MeOH (98:2). After running solvent front to within 1 cm of the top, the plates were dried and analyzed by orcinol staining. The orcinol was prepared taking 100 mg of orcinol monohydrate (Sigma-Aldrich) mixed with 12,5 ml of MEOH, 2,5 ml of ddH_2O and 5 ml of H_2SO_4 (98%). The orcinol was sprayed over the dried plates and heated to 120 °C for 5 min. After this procedure the glycolipids can be easily distinguishable as yellow spots. The spots attached to the silica were scraped from the plate and re-extracted with CH_2Cl_3:MeOH (1:1) and dried with nitrogen gas. The maximum amount of material that we got per individual plant was 10 grams. After the extraction with chloroform /methanol we got between 42 mg to 200 mg. From this material, we purified the glycolipids by using TLC-Silica from where we obtain from 20 to 250 μg of final material.

NMR

The samples were re-suspended in 1ml of CD_3OD (deuterated MeOH, NMR grade). For the analysis we used an NMR BRUKER 300MHz for 12 hrs for ^{1}H-NMR at University of Antioquia.

Mass-Spectrometry

The Mass-Spectrometry analyses were done at the University of Kansas (Mass spectrometry and analytical proteomics laboratory,1251 Wescoe Hall Lawrence, KS). Direct Infusion of glycolipid samples and acquired on a Qtof type instrument Waters Synapt G2. The samples were re-suspended in ammonium acetate (NH_4OAc) or Chloroform and methanol (2:1). We use direct infusion in negative mode with high energy fragmentation and α-GalCer (Cayman) and Monogalactosyl-Diacylglycerol (MGDG, Matreya) were used as controls for each sample analyzed (Supl. Fig. 4A and B).

B16 melanoma

To test for the activity of the lichen glycolipids we used the tumor suppression by iNKT cells in a B16 melanoma lung metastasis model. The B16 cells were grown in complete media until they reach a confluence of 70 %. B16 melanoma cells ($5x10^5$ cells /mouse) were injected into a tail vein of C57BL/6 mice, and twelve days after, the mice were sacrifice to measure the pulmonary metastasis as number of nodules per lung. Mice injected (i.p.) with the glycolipid solutions each received 0.2 ml (containing 4 μg of each glycolipid) for a glycolipid dose that was previously heated at 80 °C for 5 minutes four times, every two days after receiving the B16 melanoma.

Flow cytometry.

Antibodies to CD1d-APC, MHC class II (I-A/I-E)-FITC, CD11c-PE, CD3, Vα14-FITC and Vβ8.2-PE were purchased from BD Biosciences as fluorescent dye conjugates. Samples were analyzed using the FACS-Calibur instrument at the Albert Einstein College of Medicine, (BD Biosciences). The data was analyzed with Flowing 2.5.1 and Flowjo 7.6.

Statistical Analysis

Two way ANOVA with Bonferroni´s multiple comparisons was used for comparing groups of three or more glycolipid treatments was used to generate p values for selected pairwise comparisons, and $p < 0.05$ were considered significant. GraphPad Prism 5.0 software was used for statistical analyses. All experiments were performed in triplicate, and the results are presented as mean values with error bars representing the standard deviation (S.D.).

RESULTS

Evaluation of the iNKT cell activation by glycolipids derived from lichens

We have isolated glycolipids from a collection of different species of lichens from Colombia using a modification of the Bligh and Drier protocol and TLC (25). After the orcinol staining of the TLC plates, we were able to detect and isolate 41 glycolipids (Fig. 1A) (See methods section). To gain insight into the iNKT cells potential activity of these lichen glycolipids, we used an assay system to screen for lipid activity based on a single-TCR–specific iNKT cell hybridoma (DN3A4 1.2) that was cultured together with bone marrow derived dendritic cells BMDCs (Supl. Fig.1A, 1B). For the selection of glycolipids, we assumed positive activity for glycolipid extracts with five standard deviations above the basal activity of the negative control. Among the panel of lichen glycolipids extracts tested, only glycolipid 3 and glycolipid 26 were differentially stimulatory (Fig.1B, 1C, Supl. Fig. 3).

Glycolipid 3 is derived from de lichen *Stereocaulon ramulosum*

Once we confirm the activity of glycolipid 3 and 26 in multiple independent experiments, we decide to taxonomically classify the species of lichens from where the compounds were isolated. The glycolipid 3 comes from the lichen *Stereocaulon ramulosum* and glycolipid 26 from *Pseudocyphellaria aurata* (the classification was done with the help of Dr. Harry Sipman, Botanical Garden of Berlin, Germany and Dr. Jaime Aguirre, Instituto de Ciencias Naturales, Universidad Nacional de Colombia, Bogotá Colombia) (Fig. 1D). *S.ramulosum*, is a cosmopolitan lichen found on rocks or soil and is one of the commonest species of the *Stereocaulon* genus in Colombia. Our sample of *S.ramulosum* was found at 2400 mts of altitude in a denudated roadside bank. This lichen has a gall-like structure (cephalodia) containing blue-green algae and is characterized by a pale greyish, shrubby thallus (body of the lichen) with conspicuous red-brown apothecia (disc-like fruiting bodies) and bluish-grey warty cephalodia (Fig. 1D). On the other hand, *P. aurata* is lichen with a big distribution in the Andean mountain forests of Colombia and was found over a tree branch at 2000mts of altitude in an open area near a primary forest.

Since glycolipid 3 showed the highest activity and reproducibility, we decided to focus on this glycolipid for the rest of the paper. To see if we can obtain more glycolipid 3 from the collected material, we performed the isolation using the traditional soxhlet technique, with tree different solvents (chloroform-42, Hexane-43 and methanol-44) (Fig. 2A). We found activity with the crude extracts for chloroform and methanol (Fig. 2A). After seeing this result we decided to do a TLC with the chloroform-42 and we were able to isolate four spots (54,55,56 and 57) from which 57 gave us the highest activity (Fig. 2B), and correspond to the same spot as for glycolipid 3 with an Rf of 0,9 (data not showed). We were able to get more material from the lichens by using the soxhlet method but in terms of iNKT cell activity for glycolipid 3 there were not significant differences between the two methods that were evaluated in the paper.

The activity of glycolipid 3 is CD1d dependent

Due to the fact that iNKT cells can be activated directly by the CD1d or indirectly by cytokines, we try to determine whether the activation of the glycolipid 3 was dependent on CD1d. Remarkably, the activity of glycolipid 3 was significantly reduced when a blocking antibody (anti-CD1d) was present, suggesting a major dependence on CD1d for this glycolipid during the activation of iNKT cells (Fig. 2C). Notably, blocking the activity of CD1d for αGalCer cause a greater reduction of the production of IL-2 by the iNKT cells as compared with glycolipid 3 which could be explained by the concentration and purity of the αGalCer as compared to glycolipid 3 (Fig. 2C).

Glycolipid 3 has anti-tumor activity in vivo

Different glycolipids have been shown to promote antitumor immune responses in several cancer models trough the activation of iNKT cells (26-28). In order to determine if glycolipid 3 has in vivo activity,

we evaluate the effect of this glycolipid to control the growth of the mouse B16 melanoma. We performed an administration of αGalCer and glycolipid 3 in four doses every two days after the administration of the of B16 melanoma cells in mice. B16 melanoma cells ($5x10^5$ cells /mouse) were injected into a tail vein of C57BL/6 mice, and twelve days later, the mice were sacrifice to measure the pulmonary metastasis represented by the number of nodules per lung (Fig. 3A). As shown in Fig. 3B, αGalCer and glycolipid 3 alone, both caused a very significant decreased in the number of pulmonary metastatic foci, although the reduction of glycolipid 3 was not as significant as for αGalCer. It is possible that the administration of a-GalCer results in a more rapid and massive activation of iNKT cells and a production of typical Th1 and Th2 cytokines as compared to glycolipid 3. The other possibility is that the concentration of αGalCer could be higher as compared to the concentration of the glycolipid 3. These results could be confirmed in the future with a synthetic version of glycolipid 3.

Glycolipid 3 is a new antigen derived from *S.ramulosum* now called β-GalCer-lich

After having reproducible results that showed activity *in vitro* and *in vivo* for glycolipid 3, we did an approximation to solve its chemical structure. We subjected the glycolipid extracts to high-resolution MS where we observed one main peak at 811.4 (Fig. 4A). In order to calculate the correct molecular weight based on the MS we have to subtract an NH_4 (-18) and a hydrogen atom (-1) due to the negative mode which gave us a final molecular weight of 792.4 which is consistent with the size range of multiple reported ceramides. A set of 1D ^{1}H-NMR experiments for glycolipid 3 yielded resonances consistent with other glycolipids previously reported. The ^{1}H-NMR spectrum shows a peak R1 of 7,309 that correspond to the NH- group characteristic of a ceramide (Fig. 4B). Moreover, the spectrum shows an anomeric proton (R2 peak) with a chemical shift of 5.3 consistent with a β-linkage of the sugar to the ceramide; the group of peaks called R3 represents the sugar moiety associated with the ceramide; the groups of peaks denoted as R4 correspond to different carbons from distinct parts of the chemical structure. Finally, the group of peaks R5 represents the tails of carbons that form the ceramide (Fig.4B). Many of the structure assignments were based on the foot-printing technique and by comparisons with the ^{1}H- NMRs of the closest compound αGalCerBf (29).

We use the predictor algorithm of the software MestReNova (version 9.0.1, 2014, MestReNova Research S.L.) to obtain the possible chemical structure for glycolipid 3 applying the molecular weight and the functional groups to match the ^{1}H-NMR spectrum. Our data rely on the proton chemical shift prediction which can have great differences as compared to the ^{1}H-NMR of the natural compound due to the unpredictable dependency on average solution conformational effects, although we found very close similarities. The predicted ^{1}H-NMR spectrum shows chemical shifts (δ): 7.309, 5.346, 3.963, 3.712, 3.536, 2.665, 1.649 and 1.299 which are shared between the two spectrums (Supl. Fig. 5A). We observed more dissimilar patterns at the level of the fatty acid tails and the sugar which could be affected by some contaminants present after our glycolipid purification method.

The closest predicted ^{1}H-NMR spectrum to the one obtained for glycolipid 3, gave us a chemical structure of a β-galactosyl-ceramide with a possible C16:0 fatty acid and a C24 sphingosine that we called β-GalCer-lich (**1**) (Fig.4D). This compound has a spectrum that almost completely overlaps the NMR spectrum that was showed for glycolipid 3 (Fig. 4C).

This is in accordance with a previous report of a β-D-galactopyranosyl ceramide that was isolated from the lichen *Ramalina celastri* (11) which may originate from the algae. The most interesting feature of the glycolipid from *R. celastri* is that the most abundant fatty acids in this lichen are C16:0 with 36% and some of them with a molecular weight of 780 which is closely related to our β-GalCer-lich (**1**).

DISCUSSION

Here we identify a lichen derived glycosphingolipid antigen, β-GalCer-lich (**1**) that directly activates iNKT cells in a CD1d-restricted manner. To our knowledge, this is the first report of a lichen derived glycolipid antigen that directly activates iNKT cells, and therefore this study unveiled a new source of iNKT cell ligands. It is well known that iNKT TCRs can recognize β-linked glycolipid antigens via induced-fit molecular mimicry, in which the β-linked sugars are molded into an α-like conformation by the iNKT TCR (30-32). There are reports for β-linked glycolipids such us the glycolipid β-galactosylceramide (β-GalCer), which is structurally very similar to β-GlcCer that is also recognized by mouse and human NKT

cells, albeit with apparently lower potency than the recognition of β-GlcCer. Our β-GalCer-lich (**1**) (C16:0) is closely related to the β-GalCer (C18:0) which also exert tumor-specific cytotoxicity in vitro but has two more carbons (33, 34). It was indicated that the growth of transplanted tumors is suppressed in mice with β-ceramides with reduced fatty acid length dawn to C12, but not in those treated with β-ceramides with less carbons such us C8 (34). Another report showed results with β-GalCer C12 and β-GalCer C26 that can effectively activate iNKT cells at high concentrations in vitro and vivo similar to the prototypical αGalCer (35).

Two signals have an important role in iNKT cell activation during microbial infection: the first is a lipid antigen presented by CD1d to the iNKT cell TCR, and the second is an inflammatory cytokine, such as IL-12 (4). We did not evaluate the second alternative directly which could be present during the activation effect of our β-GalCer-lich (**1**) compound *in vivo*. Moreover, it has been showed before that αGalCer has an adjuvant effect by the induction of dendritic cell maturation, which is not seeing for other type of compounds such us αGalCerBf. To observe a good activity for our β-GalCer-lich (**1**) we have to use LPS in our in vitro experiments to mature the BMDCs if we want to get maximum activity in spite of knowing that the DN3A4 hybridoma does not respond to IL-12 derived from the treatment (36).

It would be interesting to compare if the β-GalCer-lich (**1**) is more potent that the β-GlcCer and the β-GalCer *in vitro* and *in vivo*, as the length and degree of saturation of the fatty acid tails has a considerable effect on the activity of a glycolipid antigen. This glycolipid comparison might show differences in antigen processing, glycolipid loading and TCR binding affinity. We are aware that this β-GalCer-lich (**1**) could be just an approximation to the real compound present in the lichen, and that the only way to be certain about the chemical structure is to synthetize the compound and be able to reproduce the activity as it was done for other glycolipids (37, 38).

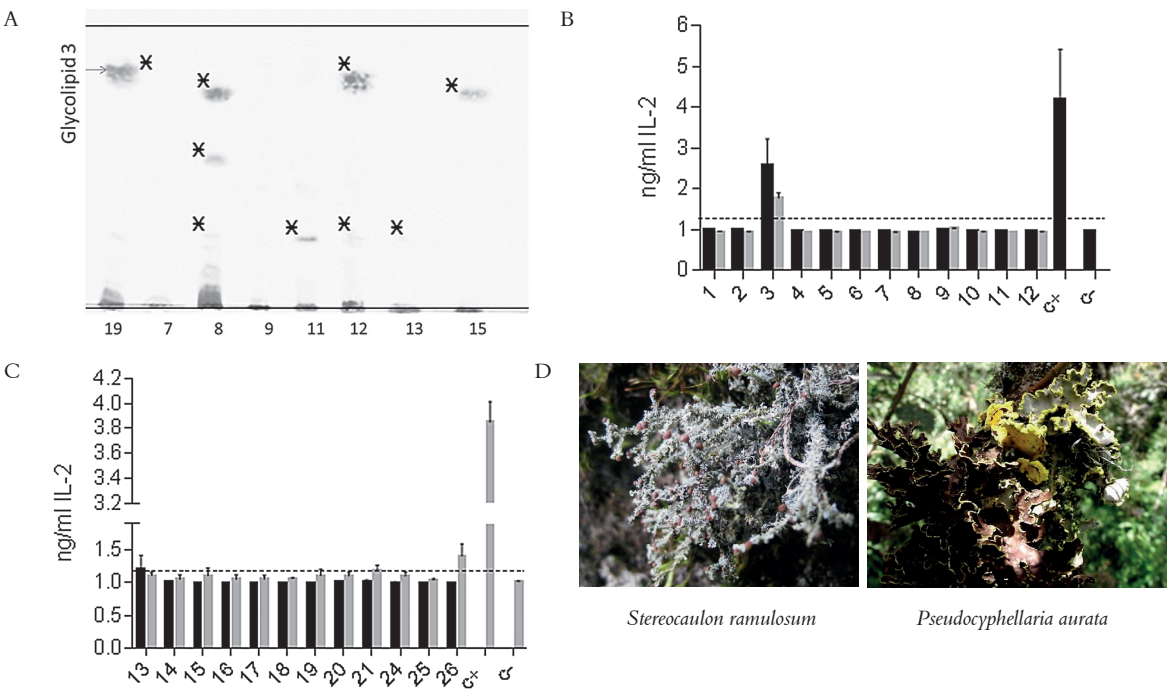

Figure 1. Identification and iNKT cell activity of glycolipids derived from lichens. **(A)** TLC of different lichen extracts showing glycolipid specific bands stained with orcinol. The arrow shows the glycolipid 3 derived from lichen 19. **(B)** In vitro activities of glycolipids 1-12 showing the production of IL-2 by the activation of the DN3A4 iNKT hybridoma (100 ng/ml of the extract in black and 200 ng/ml in grey; c(+) 120 ng/ml). **(C)** In vitro activity for glycolipids 13-26 **(D)** Pictures of the lichen species *S.ramulosum* that correspond to lichen 19 and *P.aurata* that correspond to lichen 26. Punctuated lines correspond to five standard deviations above the negative control. Experiments in B and C were repeated 3 times with 3 replicates per experiment.

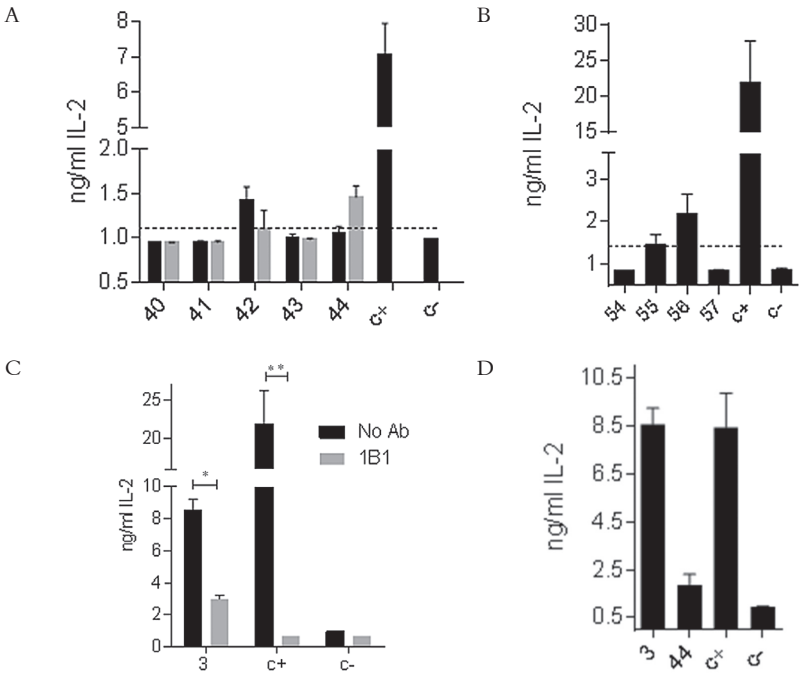

Figure 2. Specific iNKT cell activity of glycolipids derived from *S.ramulosum*. **(A)** IL-2 production by the DN3A4 iNKT hybridoma by glycolipids isolated from lichen 19 by the soxhlet method with different organis solvents (42-chloroform, 43-Hexane and 44-methanol). The positive control C (+) was αGalCer and the negative control for all experiments was DMSO. **(B)** TLC of the lichen extract 42-chloroform were we isolated specific bands after orcinol staining (54, 55, 56 and 57). Punctuated lines correspond to five standard deviations above the negative control. **(C)** Blocking of CD1d by the 1B1 antibody for glycolipid 3 and αGalCer. Inhibition of iNKT cell activity: ⋆ 98%, ⋆⋆ 66%. **(D)** Glycolipid 3 showing comparable activity with αGalCer at a lower concentration. This figure shows a representative experiment out of three with three replicate per experiment.

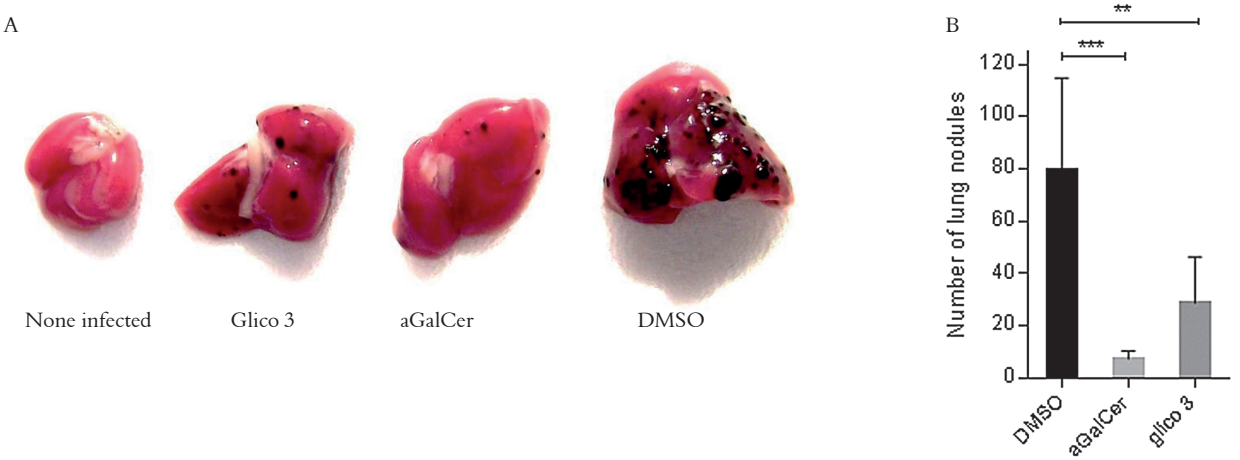

Figure 3. Tumor suppression by glycolipid iNKT cell stimulation of a B16 melanoma lung metastasis model. **(A)** Lung nodules in C57BL/6 mice 14 days after B16 melanoma intra peritoneal (i.p) injections. **(B)** Number of metastatic nodules of B16 in the lung showing the protective effect of glycolipid 3 and αGalCer (5 mice/group; 1ug per dose of Glycolipid 3 and αGalCer). Data are representative of two independent experiments. Anova ⋆<0.009 and ⋆⋆<0.0007. This is a representative of two independent experiments.

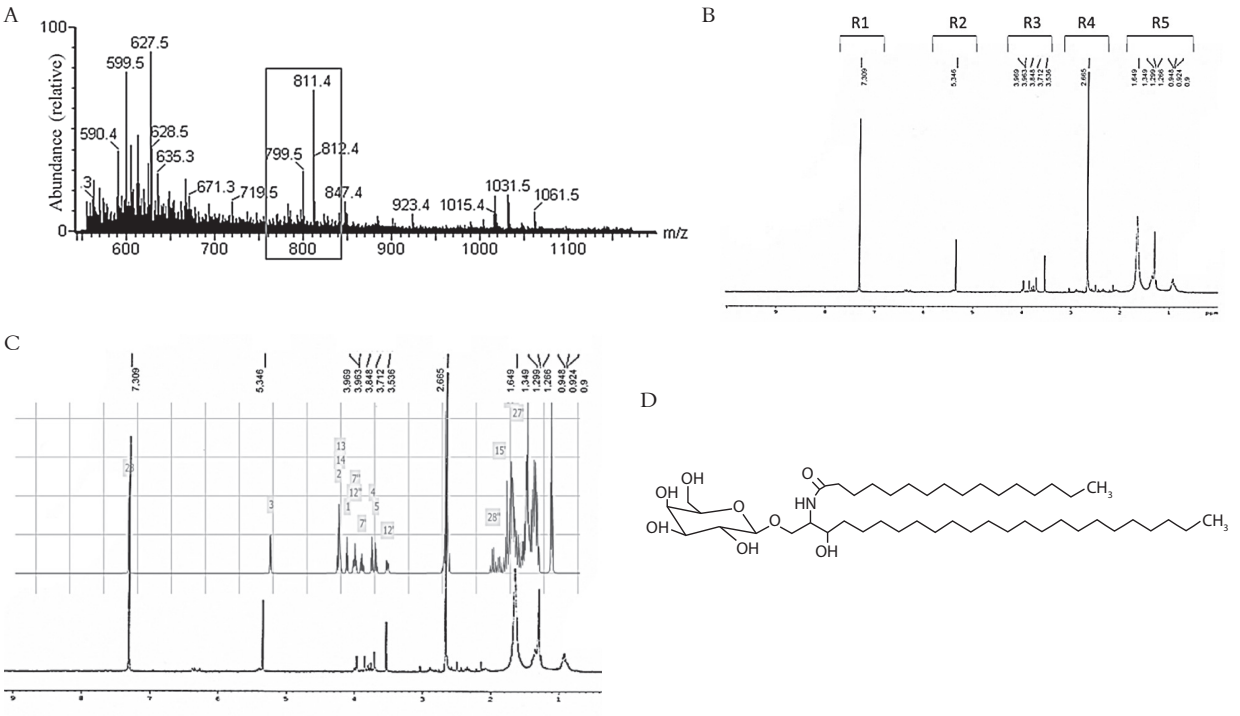

Figure 4. Chemical structure of glycolipid 3 by Mass spectrometry and NMR analysis. **(A)** Electrospray-ionization mass spectrometry analysis of glycolipid 3. m/z, mass/charge. Data are representative of two experiments. The main peak showed in the frame corresponds to the more abundant high mass compound of 811.4. **(B)** shows a representative ^{1}H NMR profile for glycolipid 3. The main peak has been grouped as regions R1, R2, R3, R4 and R5. ^{1}H NMR (300 MHz, CDCl3) δ 7.31 (s, 50H), 6.36 (d, J = 10.7 Hz, 6H), 5.37 (d, J = 12.2 Hz, 20H), 3.98 (d, J = 8.5 Hz, 11H), 3.90 – 3.66 (m, 26H), 3.54 (s, 12H), 2.89 (s, 4H), 2.79 (d, J = 17.6 Hz, 4H), 2.67 (s, 158H), 2.58 (s, 5H), 2.50 (s, 6H), 2.39 (d, J = 25.9 Hz, 11H), 2.21 (s, 4H), 2.08 (s, 14H), 2.15 – 1.25 (m, 354H), 0.91 (d, J = 7.1 Hz, 84H). **(C)** Overlay of the ^{1}H-NMR profile obtained experimentally with the predicted by MestReNova. **(D)** Chemical structure for β-GalCer-lich (**1**)

ACKNOWLEDGMENTS

We acknowledge funding from: "Programa de Sostenibilidad 2014-2015, Universidad de Antioquia" and CODI-"Programa primer Proyecto profesor vinculado-Universidad de Antioquia". We appreciate the support by all GICIG members especially with Luis F. Barrera for the advice given during the development of this project. We are in debt with Robinson Ramirez, Paula Correa and to all the other members of the GIM group for all his support with animal handling. We are grateful to Steven A. Porcelli and Leandro Carreño for the iNKT cell hybridoma. We want to thank CORANTIOQUIA for the authorization to obtain samples for this study. There is no "Conflict of interests" of authors, with the research results.

REFERENCES

1. Baena A, Porcelli SA. Evasion and subversion of antigen presentation by Mycobacterium tuberculosis. Tissue antigens. 2009 Sep;74(3):189-204.
2. Arora P, Baena A, Yu KO, Saini NK, Kharkwal SS, Goldberg MF, et al. A single subset of dendritic cells controls the cytokine bias of natural killer T cell responses to diverse glycolipid antigens. Immunity. 2014 Jan 16;40(1):105-16.
3. Carreno LJ, Kharkwal SS, Porcelli SA. Optimizing NKT cell ligands as vaccine adjuvants. Immunotherapy. 2014 Mar;6(3):309-20.
4. Brennan PJ, Brigl M, Brenner MB. Invariant natural killer T cells: an innate activation scheme linked to diverse effector functions. Nature reviews Immunology. 2013 Feb;13(2):101-17.
5. Rappuoli R, Aderem A. A 2020 vision for vaccines against HIV, tuberculosis and malaria. Nature. 2011 May 26;473(7348):463-9.
6. Koff WC, Burton DR, Johnson PR, Walker BD, King CR, Nabel GJ, et al. Accelerating next-generation vaccine development for global disease prevention. Science. 2013 May 31;340(6136):1232910.

7. Rey-Ladino J, Ross AG, Cripps AW, McManus DP, Quinn R. Natural products and the search for novel vaccine adjuvants. Vaccine. 2011 Sep 2;29(38):6464-71.
8. Muller K. Pharmaceutically relevant metabolites from lichens. Appl Microbiol Biot. 2001 Jul;56(1-2):9-16.
9. Temina M, Levitsky DO, Dembitsky VM. Chemical Constituents of the Epiphytic and Lithophilic Lichens of the Genus Collema. Rec Nat Prod. 2010;4(1):79-86.
10. Sassaki GL, Gorin PA, Reis RA, Serrato RV, Elifio SL, Iacomini M. Carbohydrate, glycolipid, and lipid components from the photobiont (Scytonema sp.) of the lichen, Dictyomema glabratum. Carbohydrate research. 2005 Aug 15;340(11):1808-17.
11. Machado MJ, Guerrini M, Gorin PAJ, Torri G, Iacomini M. A galactosphingolipid from the lichen, Ramalina celastri. Phytochemistry. 1997 Jun;45(4):651-3.
12. Kotlova ER, Sinyutina NF. Change's in the content of individual lipid classes of a lichen Peltigera aphthosa during dehydration and subsequent rehydration. Russ J Plant Physl+. 2005 Jan-Feb;52(1):35-42.
13. Bychek IA, Bychek EA. Comparison of lipids and fatty acids of the lichen Rhizoplaca peltata collected from foothill and high mountain habitats in the same region. Lichenologist. 1996 Sep;28:465-9.
14. Arora P, Venkataswamy MM, Baena A, Bricard G, Li Q, Veerapen N, et al. A rapid fluorescence-based assay for classification of iNKT cell activating glycolipids. Journal of the American Chemical Society. 2011 Apr 13;133(14):5198-201.
15. Natori T, Koezuka Y, Higa T. Agelasphins, Novel Alpha-Galactosylceramides from the Marine Sponge Agelas-Mauritianus. Tetrahedron Lett. 1993 Aug 27;34(35):5591-2.
16. Natori T, Morita M, Akimoto K, Koezuka Y. Agelasphins, Novel Antitumor and Immunostimulatory Cerebrosides from the Marine Sponge Agelas-Mauritianus. Tetrahedron. 1994 Feb 28;50(9):2771-84.
17. Gordien AY, Gray AI, Ingleby K, Franzblau SG, Seidel V. Activity of Scottish plant, lichen and fungal endophyte extracts against Mycobacterium aurum and Mycobacterium tuberculosis. Phytother Res. 2010 May;24(5):692-8.
18. Ingolfsdottir K, Chung GA, Skulason VG, Gissurarson SR, Vilhelmsdottir M. Antimycobacterial activity of lichen metabolites in vitro. European journal of pharmaceutical sciences : official journal of the European Federation for Pharmaceutical Sciences. 1998 Apr;6(2):141-4.
19. Garcia A, Bocanegra-Garcia V, Palma-Nicolas JP, Rivera G. Recent advances in antitubercular natural products. Eur J Med Chem. 2012 Mar;49:1-23.
20. Rankovic B, Misic M, Sukdolak S. Antimicrobial activity of extracts of the lichens Cladonia furcata, Parmelia caperata, Parmelia pertusa, Hypogymnia physodes and Umbilicaria polyphylla. Biologia. 2009 Feb;64(1):53-8.
21. Gordien AY, Gray AI, Ingleby K, Franzblau SG, Seidel V. Activity of Scottish Plant, Lichen and Fungal Endophyte Extracts against Mycobacterium aurum and Mycobacterium tuberculosis. Phytother Res. 2010 May;24(5):692-8.
22. Mateus N, Aguirre J, Lucking R. Contributions to the Foliicolous Lichen biota of Choco (Colombia). Caldasia. 2012 Jun 30;34(1):25-32.
23. Rincon-Espitia A, Aguirre J, Lucking R. Corticolous lichens in the Caribbean region of Colombia. Caldasia. 2011;33(2):331-47.
24. Lutz MB, Kukutsch N, Ogilvie AL, Rossner S, Koch F, Romani N, et al. An advanced culture method for generating large quantities of highly pure dendritic cells from mouse bone marrow. Journal of immunological methods. 1999 Feb 1;223(1):77-92.
25. Iverson SJ, Lang SL, Cooper MH. Comparison of the Bligh and Dyer and Folch methods for total lipid determination in a broad range of marine tissue. Lipids. 2001 Nov;36(11):1283-7.
26. Nishio S, Yamada N, Ohyama H, Yamanegi K, Nakasho K, Hata M, et al. Enhanced suppression of pulmonary metastasis of malignant melanoma cells by combined administration of alpha-galactosylceramide and interleukin-18. Cancer science. 2008 Jan;99(1):113-20.
27. Aspeslagh S, Nemcovic M, Pauwels N, Venken K, Wang J, Van Calenbergh S, et al. Enhanced TCR footprint by a novel glycolipid increases NKT-dependent tumor protection. Journal of immunology. 2013 Sep 15;191(6):2916-25.
28. Aspeslagh S, Li Y, Yu ED, Pauwels N, Trappeniers M, Girardi E, et al. Galactose-modified iNKT cell agonists stabilized by an induced fit of CD1d prevent tumour metastasis. The EMBO journal. 2011 Jun 1;30(11):2294-305.
29. Wieland Brown LC, Penaranda C, Kashyap PC, Williams BB, Clardy J, Kronenberg M, et al. Production of alpha-galactosylceramide by a prominent member of the human gut microbiota. PLoS biology. 2013 Jul;11(7):e1001610.
30. Tsuji M. Glycolipids and phospholipids as natural CD1d-binding NKT cell ligands. Cellular and molecular life sciences : CMLS. 2006 Aug;63(16):1889-98.
31. Parekh VV, Singh AK, Wilson MT, Olivares-Villagomez D, Bezbradica JS, Inazawa H, et al. Quantitative and qualitative differences in the in vivo response of NKT cells to distinct alpha- and beta-anomeric glycolipids. Journal of immunology. 2004 Sep 15;173(6):3693-706.
32. Pei B, Vela JL, Zajonc D, Kronenberg M. Interplay between carbohydrate and lipid in recognition of glycolipid antigens by natural killer T cells. Annals of the New York Academy of Sciences. 2012 Apr;1253:68-79.
33. Brennan PJ, Tatituri RV, Brigl M, Kim EY, Tuli A, Sanderson JP, et al. Invariant natural killer T cells recognize lipid self antigen induced by microbial danger signals. Nature immunology. 2011 Dec;12(12):1202-11.
34. Inafuku M, Li C, Kanda Y, Kawamura T, Takeda K, Oku H, et al. Beta-glucosylceramide administration (i.p.) activates natural killer T cells in vivo and prevents tumor metastasis in mice. Lipids. 2012 Jun;47(6):581-91.
35. Oku H, Li C, Shimatani M, Iwasaki H, Toda T, Okabe T, et al. Tumor specific cytotoxicity of beta-glucosylceramide: structure-cytotoxicity relationship and anti-tumor activity in vivo. Cancer chemotherapy and pharmacology. 2009 Aug;64(3):485-96.
36. Wingender G, Rogers P, Batzer G, Lee MS, Bai D, Pei B, et al. Invariant NKT cells are required for airway inflammation induced by environmental antigens. The Journal of experimental medicine. 2011 Jun 6;208(6):1151-62.
37. Kinjo Y, Tupin E, Wu D, Fujio M, Garcia-Navarro R, Benhnia MR, et al. Natural killer T cells recognize diacylglycerol antigens from pathogenic bacteria. Nature immunology. 2006 Sep;7(9):978-86.
38. Kinjo Y, Illarionov P, Vela JL, Pei B, Girardi E, Li X, et al. Invariant natural killer T cells recognize glycolipids from pathogenic Gram-positive bacteria. Nature immunology. 2011 Oct;12(10):966-74.

SUPPLEMENTARY MATERIALS

Supplementary figure 1. (A) Flow cytometry analysis of BMDCs with and without LPS using the CD11c-PE and I-A/I-E-FITC antibodies **(B)** Flow cytometry analysis of the DN3A4 1.2 hybridoma used in the different experiments using the Vα14-FITC and the Vβ8.2-PE.

A

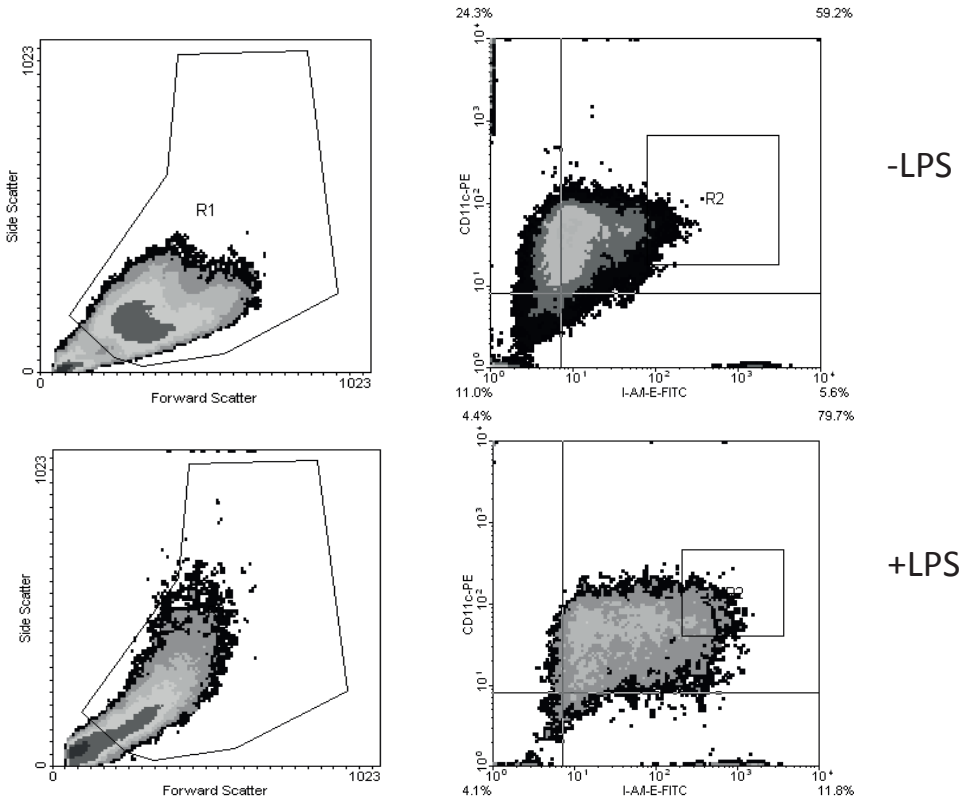

B

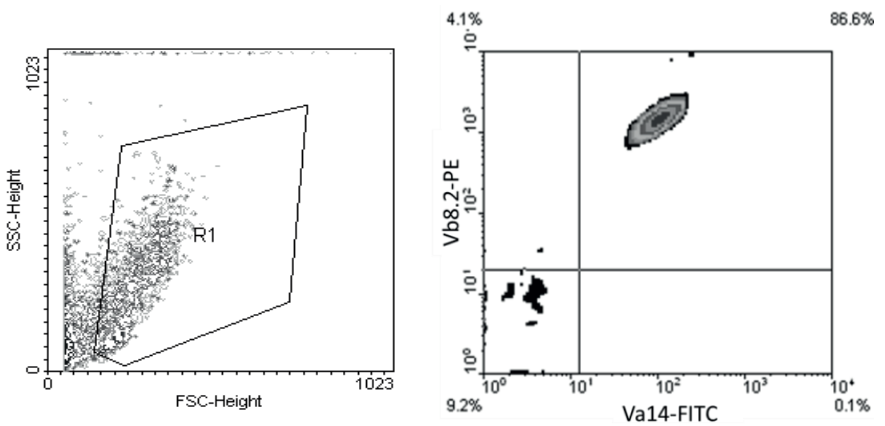

Supplementary figure 2. (A) IL-2 standard curve for figure 1B. **(B)** IL-2 standard curve for figure 1C. **(C)** IL-2 standard curve for figure 2A. **(D)** IL-2 standard curve for figure 2B. The IL-2 production in ng/ml was calculated by a regression fit curve using the software Prism 6.

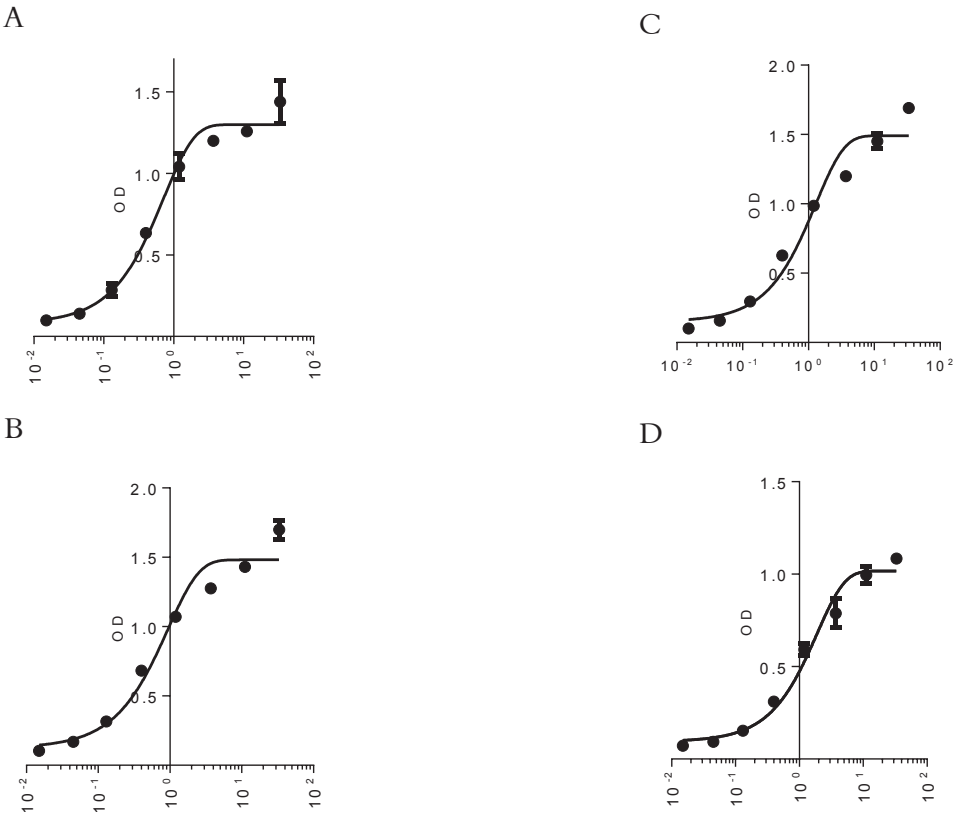

Supplementary figure 3. (A) In vitro activities of glycolipids 27-31 showing the production of IL-2 by the activation of the DN3A4 iNKT hybridoma. **(B)** In vitro activities of glycolipids 32-41. Black bars 500ng/ml and grey bars 1ug/ml. αGalCer was used as positive control (100ng/ml).

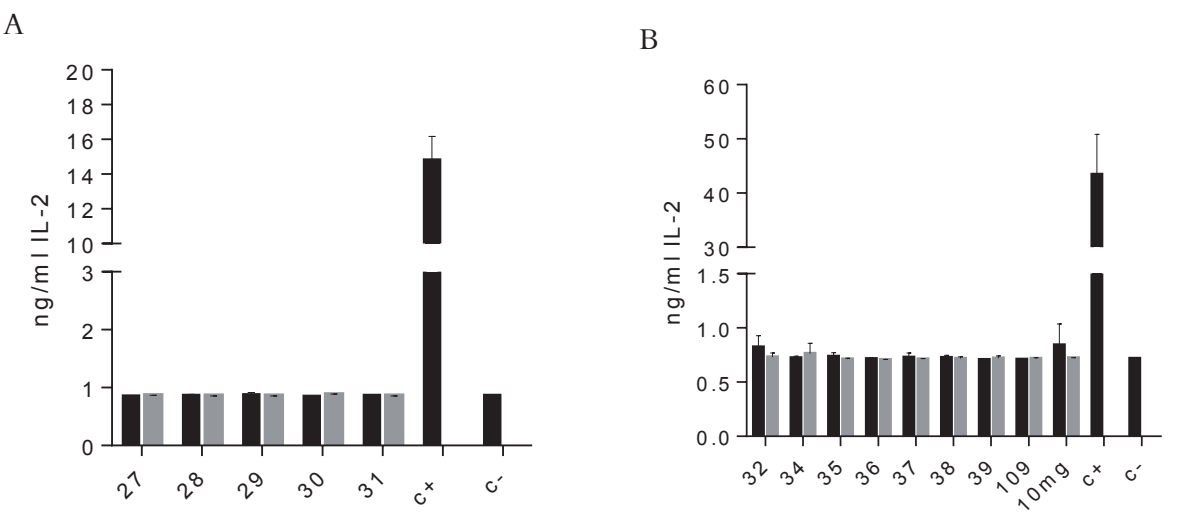

Supplementary figure 4. (A) Mass spectrometry analysis for αGalCer. **(B)** Mass spectrometry analysis for MGDG.

A

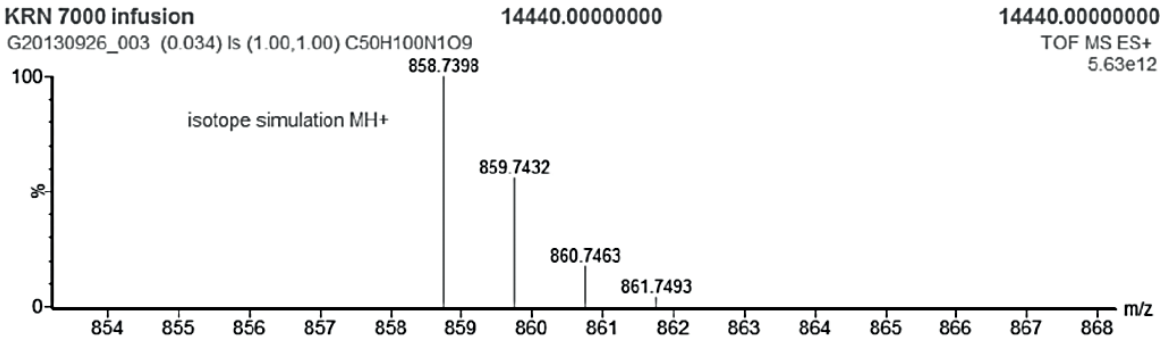

B

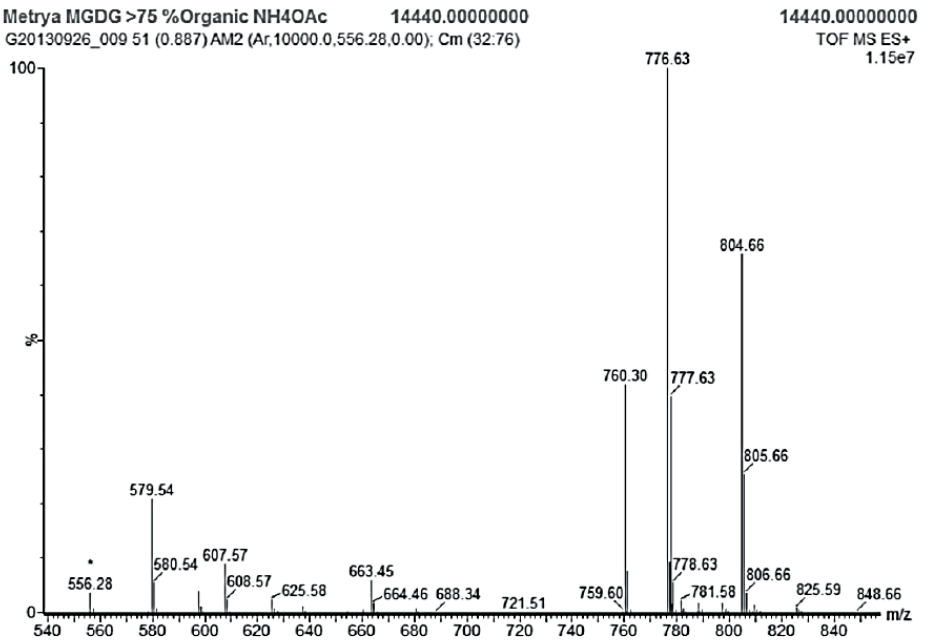

Supplementary figure 5. (A) MestReNova prediction analysis for glycolipid 3, detailing the chemical structure for glycolipid 3 now called β-GalCer-lich [1]. (B) 1H NMR data for the predicted β-GalCer-lich [1] compound.

A

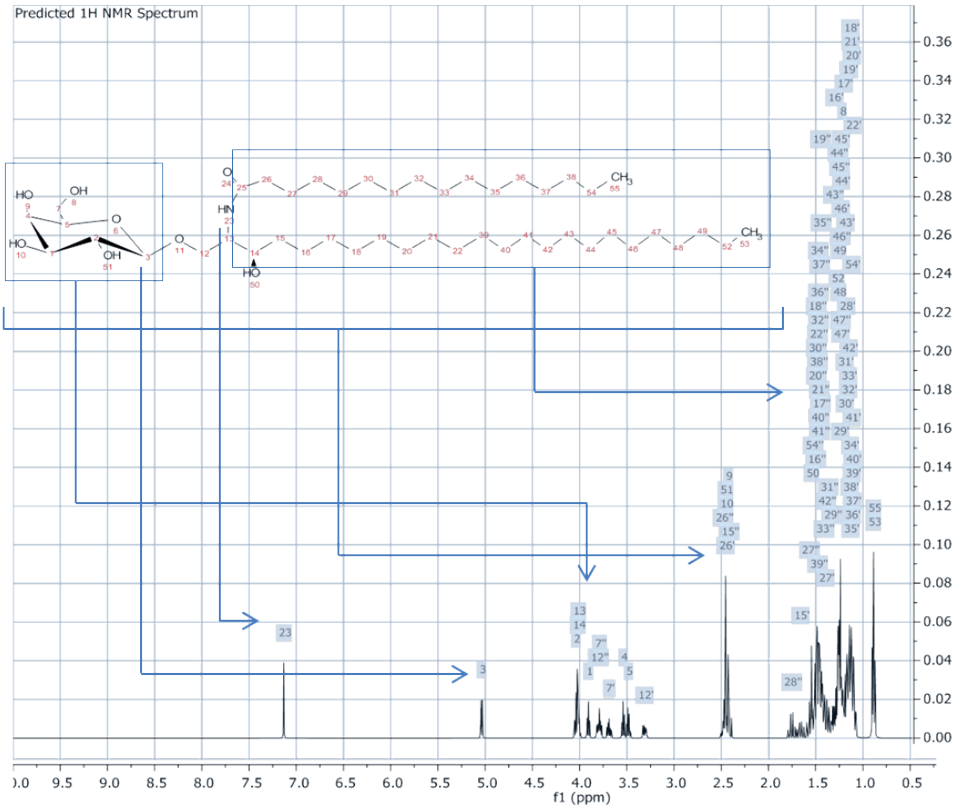

B

^{1}H NMR (500.130 MHz, Chloroform-d)

Position	Type	δ ^{1}H (error)	J(atom; Hz)
1	CH	3.91 (0.55)	J(1-2; 7.0), J(1-4; 7.0)
2	CH	4.04 (0,9)	J(2-51; 5.0)
3	CH	5.32 (0.5)	J(3-2; 7.0)
4	CH	3.54 (0.3)	J(4-5; 7.0)
5	CH	3.49 (0.35)	J(5-7'; 7.0)
7'	CH2	3.69 (0.45)	J(7'-7''; -12.40), J(7'-8; 5.50)
7''	CH2	3.79 (0.45)	J(7''-5; 7.0)
8	OH	1,23 (0.5)	J(7''-8; 5.50)
9	OH	2.58 (0,5)	J(9-4; 5.0)
10	OH	2.58 (0.5)	J(10-1; 5.0)
12'	CH2	3.31 (0.5)	J(12'-12''; -12.4), J(12'-13;7.0)
12''	CH2	3.8 (0.5)	J(12''-13;7.0)
13	CH	4.02 (0.7)	J(13-14; 7.0), J(13-15';-0.18), J(13-15''; 0.23)
14	CH	4.02 (0.7)	J(14-15',10.87), J(14-15'', 0.99), J(14-16', 3.02), J(14-50; 5.0)
15'	CH2	1.66 (0.7)	J(15'-15''; -12.4), J(15'-16'; 3.02), J(15'-16''; 13.18), J(15'-17'; -0.22), J(15'-17'';-0.19)
15''	CH2	2.58 (0.7)	J(15''-16', 13.15), J(15''-16'', 2.06), J(15''-17', -0.11), J(15''-17'', -0.08)
16'	CH2	1.30 (0.7)	J(16'-16''; -12.40), J(16'-17', 2.61), J(16'-17'', 13.21), J(16'-18', -0.16), J(16'-18''; -0.18)
16''	CH2	1.5 (0.7)	J(16''-17',13.21), J(16''-17'', 2.42), J(16''-18',-0.14), J(16''-18'', -0.15)
17'	CH2	1.2 (0.7)	J(17'-17''; -12.40), J(17'-18', 2.46), J(17'-18'' 13.21), J(17'-19';-0.14), J(17'-19'';-0.16)
17''	CH2	1.45 (0.7)	J(17''-18', 13.21), J(17''-18'', 2.59), J(17''-19', -0.16), J(17''-19'';-0.17)
18'	CH2	1.13 (0.35)	J(18'-18''; -12.4), J(18'-19'; 2.47), J(18'-19''; 13.21), J(18'-20'; -0.13), J(18'-20''; -0.17)
18''	CH2	1.5 (0.35)	J(18''-19';13.21), J(18''-19'', 2.57), J(18''-20', -0.15), J(18''-20'', -0.18)
19'	CH2	1.15 (0.3)	J(19'-19''; -12.40), J(19'-20', 2.39), J(19'-20'' 13.21), J(19'-21'; -0.13), J(19'-21''; -0.15)
19''	CH2	1.45 (0.3)	J(19''-20' 13.21), J(19''-20'', 2.66), J(19''-21', -0.17), J(19''-21'', -0.18)
20'	CH2	1.12 (0.3)	J(20'-20''; -12.4), J(20'-21'; 2.47), J(20'-21''; 13.21), J(20'-22'; -0.14), J(20'-22''; -0.16)
20''	CH2	1.50 (0.3)	J(20''-21'; 13.21), J(20''-21'', 2.58), J(20''-22'; -0.15), J(20''-22''; -0.18)
21'	CH2	1.14 (0.3)	J(21'-21''; -12.4), J(21'-22'; 2.43), J(21'-22''; 13.21), J(21'-39'; -0.15), J(21'-39''; -0.14)
21''	CH2	1.47 (0.3)	J(21''-22'; 13.21), J(21''-22'', 2.62), J(21''-39'; -0.17), J(21''-39''; -0.17)
22'	CH2	1.11 (0.3)	J(22'-22''; -12.40), J(22'-39', 2.55), J(22'-39'' 13.21), J(22'-40'; -0.16), J(22'-40''; -0.16)
22''	CH2	1.49 (0.3)	J(22''-39'; 13.21), J(22''-39'', 2.50), J(22''-40'; -0.15), J(22''-40''; -0.16)
23	CH2	7.30 (0.5)	
26'	CH2	2.56 (0.7)	J(26'-26''; -12.4), J(26'-27'; 10.36), J(26'-27''; 4.91), J(26'-28'; -0.40), J(26'-28''; -0.15)
26''	CH2	2.59 (0.7)	J(26''-27', 5.33), J(26''-27'', 3.79), J(26''-28', 0.45), J(26''-28'', 0.70)
27'	CH2	1.40 (0.5)	J(27'-27''; -12.4), J(27'-28', 3.92), J(27'-28'' 12.92), J(27'-29', -0.38), J(27'-29'' -0.19)
27''	CH2	1.57 (0.5)	J(27''-28', 12.79), J(27''-28'', 1.30), J(27''-29', -0.06), J(27''-29'', 0.13)
28'	CH2	1.18 (0.35)	J(28'-28''; -12.4), J(28'-29'; 3.37), J(28'-29'' 13.10), J(28'-30'; -0.32), J(28'-30''; -0.17)
28''	CH2	1.76 (0.35)	J(28''-29', 13.08), J(28''-29'', 1.77), J(28''-30', -0.12), J(28''-30'', 0.03)
29'	CH2	1.24 (0.3)	J(29'-29''; -12.4), J(29'-30'; 3.17), J(29'-30'' 13.14), J(29'-31'; -0.27), J(29'-31''; -0.18)
29''	CH2	1.34 (0.3)	J(29''-30', 13.14), J(29''-30'', 1.96), J(29''-31', -0.13), J(29''-31'', -0.03)
30'	CH2	1.19 (0.3)	J(30'-30''; -12.40), J(30'-31', 2.91), J(30'-31'' 13.18), J(30'-32'; -0.23), J(30'-32''; -0.17)
30''	CH2	1.50 (0.3)	J(30''-31', 13,18), J(30''-31'', 2.17), J(30''-32', -0.14), J(30''-32'', -0.08)
31'	CH2	1.20 (0.3)	J(31'-31''; -12.40), J(31'-32', 2.78), J(31'-32'' 13.20), J(31'-33'; -0.20), J(31-33''; -0.17)
31''	CH2	1.37 (0.3)	J(31''-32', 13.20), J(31''-32'', 2.29), J(31''-33', -0.14), J(31''-33'', -0.11)
32'	CH2	1.16 (0.3)	J(32'-32''; -12.4), J(32'-33'; 2.67), J(32'-33'' 13.21), J(32'-34';-0.19), J(32'-34''; -0.16)
32''	CH2	1.47 (0.3)	J(32''-33'; 13.21), J(32''-33'', 2.39), J(32''-34'; -0.15), J(32''-34''; -0.13)
33'	CH2	1.16 (0.3)	J(33'-33''; -12.4), J(33'-34', 2.61), J(33'-34'' 13.21), J(33'-35'; -0.17), J(33'-35''; -0.16)
33''	CH2	1.42 (0.3)	J(33''-34', 13.21), J(33''-34'', 2.44), J(33''-35'; -0.15), J(33''-35''; -0.14)
34'	CH2	1.14 (0.3)	J(34'-34''; -12.4), J(34'-35', 2.58), J(34'-35'' 13.21), J(34'-36'; -0.17), J(34'-36''; -0.16)

^{1}H NMR (500.130 MHz, Chloroform-d)

Position	Type	δ ^{1}H (error)	J(atom; Hz)
34''	CH2	1.48 (0.3)	J(34''-35'; 13.21), J(34''-35''; 2.47), J(34''-36'; -0.16), J(34''-36'';-0.15)
35'	CH2	1.13 (0.3)	J(35'-35''; -12.40), J(35'-36', 2.57), J(35'-36'' 13.21), J(35'-37'; -0.17), J(35'-37''; -0.16)
35''	CH2	1.45 (0.3)	J(35''-36', 13.21), J(35''-36'', 2.48), J(35''-37'; -0.16), J(35''-37''; -0.15)
36'	CH2	1.13 (0.3)	J(36'-36''; -12.40), J(36'-37', 2.57), J(36'-37'' 13.21), J(36''-38'; -0.17), J(36''-38''; -0.16)
36''	CH2	1.47 (0.3)	J(36''-37'; 13.21), J(36''-37'', 2.47), J(36''-38'; -0.16), J(36''-38''; -0.15)
37'	CH2	1.12 (0.3)	J(37'-37''; -12.40), J(37'-38', 2.59), J(37'-38'' 13.21), J(37''-54'; -0.17), J(37''-54''; -0.16)
37''	CH2	1.46 (0.3)	J(37''-38', 13.21), J(37''-38'', 2.45), J(37''-54'; -0.16), J(37''-54''; -0.15)
38'	CH2	1.14 (0.3)	J(38'-38''; -12.40), J(38'-54', 2.61), J(38'-54'' 13.21)
38''	CH2	1.48 (0.3)	J(38''-54' 13.21), J(38''-54'' 2.49)
39'	CH2	1.12 (0.3)	J(39'-39''; -12.40), J(39'-40', 2.50), J(39'-40'' 13.21), J(39'-41'; -0.17), J(39'-41''; -0.14)
39''	CH2	1.48 (0.3)	J(39''-40', 13.21), J(39''-40'', 2.54), J(39''-41'; -0.18), J(39''-41''; -0.15)
40'	CH2	1.12 (0.3)	J(40'-40''; -12.40), J(40'-41', 2.66), J(40'-41'' 13.21), J(40'-42'; -0.18), J(40'-42''; -0.17)
40''	CH2	1.47 (0.3)	J(40''-41', 13.21), J(40''-41'', 2.39), J(40''-42'; -0.15), J(40''-42''; -0.14)
41'	CH2	1.12 (0.3)	J(41'-41''; -12.40), J(41'-42', 2.56), J(41'-42'' 13.21), J(41'-43'; -0.18), J(41'-43''; -0.14)
41''	CH2	1.46 (0.3)	J(41''-42', 13.21), J(41''-42'', 2.48), J(41''-43'; -0.17), J(41''-43''; -0.13)
42'	CH2	1.15 (0.3)	J(42'-42''; -12.40), J(42'-43', 2.72), J(42'-43'' 13.20), J(42'-44'; -0.18), J(42'-44''; -0.18)
42''	CH2	1.40 (0.3)	J(42''-43', 13.20), J(42''-43'', 2.33), J(42''-44'; -0.14), J(42''-44''; -0.15)
43'	CH2	1.19 (0.3)	J(43'-43''; -12.40), J(43'-44', 2.55), J(43'-44'' 13.21), J(43'-45'; -0.16), J(43'-45''; -0.16)
43''	CH2	1.31 (0.3)	J(43''-44', 13.21), J(43''-44'', 2.50), J(43''-45'; -0.16), J(43''-45''; -0.15)
44'	CH2	1.23 (0.3)	J(44'-44''; -12.40), J(44'-45', 2.53), J(44'-45'' 13.21), J(44'-46'; -0.16), J(44'-46''; -0.16)
44''	CH2	1.27 (0.3)	J(44''-45', 13.21), J(44''-45'', 2.53), J(44''-46'; -0.16), J(44''-46''; -0.16)
45'	CH2	1.24 (0.3)	J(45'-45''; -12.40), J(45'-46', 2.53), J(45'-46'' 13.21), J(45'-47'; -0.16), J(45'-47''; -0.16)
45''	CH2	1.25 (0.3)	J(45''-46', 13.21), J(45''-46'', 2.53), J(45''-47'; -0.16), J(45''-47'';-0.16)
46'	CH2	1.24 (0.3)	J(46'-46''; -12.40), J(46'-47', 2.53), J(46'-47'' 13.21), J(46'-48'; -0.16), J(46'-48''; -0.16)
46''	CH2	1.24 (0.3)	J(46''-47', 13.21), J(46''-47'', 2.53), J(46''-48'; -0.16), J(46''-48''; -0.16)
47'	CH2	1.24 (0.3)	J(47'-47''; -12.40), J(47'-48', 2.53), J(47'-48'' 13.21), J(47'-49'; -0.16), J(47'-49'';-0.16)
47''	CH2	1.24 (0.3)	J(47''-48', 13.21), J(47''-48'', 2.53), J(47''-49'; -0.16), J(47''-49''; -0.16)
48'	CH2	1.23 (0.3)	J(48'-48''; -12.40), J(48'-49', 2.53), J(48'-49'' 13.21), J(48'-52'; -0.16), J(48'-52''; -0.16)
48''	CH2	1.23 (0.3)	J(48''-49', 13.21), J(48''-49'', 2.53), J(48''-52'; -0.16), J(48''-52''; -0.16)
49'	CH2	1.26 (0.3)	J(49'-49''; -12.40), J(49'-52', 2.56), J(49'-52'' 13.21)
49''	CH2	1.26 (0.3)	J(49''-52', 13.21), J(49''-52'', 2.56)
50	OH	1.55 (0.5)	J(50-14; 5.0)
51	OH	2.56 (0.5)	J(51-2, 5.0)
52'	CH2	1.27 (0.2)	J(52'-52'';-12.40), J(52'-53; 8.0)
52''	CH2	1.27 (0.2)	J(52''-53; 8.0)
53	CH3	0.89 (0.2)	J(53; -12.50)
54'	CH2	1.13 (0.2)	J(54'-54''; -12.40), J(54'-55; 8.0)
54''	CH2	1.53 (0.2)	J(54''-55; 8.0)
55	CH3	0.89 (0.2)	J(55; -12.50)